ADVANCED FUNCTIONAL MATERIALS

FULL PAPER

DOI: 10.1002/adfm.200500568

Engineering Increased Stability into Self-Assembled Protein Fibers**

By *Andrew M. Smith*, *Eleanor F. Banwell*, *Wayne R. Edwards*, *Maya J. Pandya*, and *Derek N. Woolfson**

Two stages in the rational redesign of a peptide-based, self-assembling fiber (SAF) are described. The SAF system comprises two peptides designed to form an offset α-helical coiled-coil heterodimer. The "sticky-ends" are complementary and promote longitudinal assembly. Alone, the two peptides are unstructured, but co-assemble upon mixing to form α-helical fibrils, which bundle to form fibers 40–50 nm wide and tens of micrometers long. Assembly is controllable and occurs at pH 7 in water, making SAFs a potential scaffold for 3D cell culture. The purposes of the redesigns were 1) to investigate the fiber-thickening process, and 2) to increase fiber stability for potential biological and biomedical applications. First, mutations were made to the original peptide designs to increase fibril–fibril interactions and so produce thicker and more-stable fibers. The second iteration aimed to increase the primary peptide–peptide interactions by increasing the overlap in the offset dimer and so promote the initial step in fiber formation. As judged by circular dichroism spectroscopy and transmission electron microscopy, both iterations improved fiber assembly and stability: the critical peptide concentration for assembly improved from 60 μM to 4 μM; the midpoint of thermal unfolding increased from 22 °C to 65 °C; and the salt tolerance improved from 75 mM to greater than 250 mM KCl. These improvements bring closer applications of the SAF system under physiological conditions, for example as a biocompatible material for 3D cell culture. In addition, ordered surface features were observed in the second- and third-generation fibers compared with the original design. This indicates improved internal order in the redesigned fibers. In turn, this suggests a molecular mechanism for the improved stability and sheds light on the fiber-assembly process.

1. Introduction

The design and engineering of self-assembled peptide-based materials is receiving increasing attention in materials science.[1,2] This is partly because of the inspiration that biological materials provide to materials scientists; our improved ability to design, engineer and characterize peptides and proteins in general over the past decade; and the variety of potential applications for such materials in the broad areas of bionanotechnology and biotechnology. Potential applications for self-assembled peptide systems include components of smart and responsive materials, as biocompatible materials for surface engineering, and as templates for the growth and organization of organic and inorganic materials.[1,2] One specific application is as a scaffolds for 3D cell culture and tissue engineering (TE).[3]

TE is a multidisciplinary field that encompasses aspects of chemistry, cell biology, and engineering. The ultimate aim of TE is to produce 3D cell cultures and fully functional tissues for applications in regenerative medicine. The current state-of-the-art is to use biodegradable materials (often described as scaffolds)—which can either be preformed or assembled in situ—in combination with cells, with cell culture often being carried out in a bioreactor.[4,5] Ideally, in this way, the combination of support, cell type, and conditions can be chosen to direct differentiation of cells down one lineage and, thence, the production of one tissue type. Our interest in this area has to been to design self-assembling, biocompatible materials for development as scaffolds for 3D cell culture.

Gene expression in cells has been known for some time to be linked not only to chemical composition, but also to surface topography of scaffolds.[6] Consequently, for 3D cell culture to be successful, scaffolds must mimic the native extracellular matrix (ECM) as far as possible. There is a vast array of available scaffolds for tissue engineering; they range from solid pre-formed polymer scaffolds, formed using heat fusion or adhesive techniques, to cell/scaffold hybrids with assembly of the scaffold encapsulating the cells.[7] The native ECM is predominantly composed of a nonwoven mesh of fibrous proteins, such as collagen

[*] Prof. D. N. Woolfson,[+,++] Dr. A. M. Smith,[+++] E. F. Banwell,[+] Dr. W. R. Edwards,[++++] Dr. M. J. Pandya[+++++]
Department of Biochemistry, School of Life Sciences
University of Sussex
Falmer, BN1 9QG (UK)
E-mail: d.n.woolfson@bristol.ac.uk

[+] Current address: School of Chemistry, University of Bristol, Bristol BS8 1TS, UK.

[++] Current address: Department of Biochemistry, The School of Medical Sciences, University of Bristol, University Walk, Bristol BS8 1TD, UK.

[+++] Current address: School of Biochemistry and Molecular Biology, University of Leeds, Leeds LS2 9JT, UK.

[++++] Current address: Centre for Biomolecular Sciences, University of Nottingham, University Park, Nottingham NG7 2RD, UK.

[+++++] Current address: TU Munich, Lehrstuhl Biotech IV, Department Chemie, 85747 Garching, Germany.

[**] We thank Dr. Max Ryadnov for the preparation of synthetic peptide and his insightful comments on this work and its presentation in this manuscript. The work was supported by grants from the BBSRC, EPSRC and MRC of the UK (E13753 and G0300539).

ADVANCED FUNCTIONAL MATERIALS

and elastin, that provide tensile strength and elasticity. For this reason fibrous scaffolds on a similar scale to the fibrous proteins in native ECM are of particular interest. The most common fibrous scaffolds are polymer based and are often electrospun. This method is comparatively cheap and allows production of both randomly orientated and aligned scaffolds with fibers of controllable width on the same scale as the fibers in native ECM.[8] In contrast, we are interested in developing self-assembling peptide systems for TE applications. In principle, the structures and stabilities of self-assembled materials can be programmed into their molecular building blocks,[9] i.e., from the bottom up. There is currently a lot of interest in this approach as peptides and proteins have several potential advantages over alternative scaffold materials:[10–12] native ECMs have a large protein component; peptides are relatively easy to produce, either synthetically or recombinantly; and, in principle, peptides can be assembled in the presence of cells, allowing encapsulation and avoiding the problem of stimulating ingrowth into preformed scaffolds. Peptide-based self-assembling systems capable of supporting cell growth have been produced. For example, Holmes et al. have designed a β-sheet-based peptide that forms gels that can encapsulate cells.[13] Hartgerink et al. have designed a peptide-amphiphile-based self-assembling fibrous system that gels under acidic conditions.[14] This comprises a hydrophobic alkyl tail and polar amino acid head group that includes the RGD (arginine–glycine–aspartic acid) cell-attachment sequence. This has been used to foster the growth of bone in vitro.[15] The same group has also succeeded in differentiating neural-progenitor cells into neurons on a peptide-amphiphile scaffold incorporating the neurite-promoting laminin epitope IKVAV.[16] Most recently, Schneider and coworkers reported interactions between cells and a self-supporting gel formed from a self-assembling β-hairpin peptide.[17] The design and assembly of biomaterials of this type and their application in TE is described more fully in several contemporary reviews.[1,2,18,19]

Previously, we have designed a self-assembling fiber (SAF) system based on the relatively well-understood leucine-zipper motif.[20] The leucine zipper is the most straightforward example of the α-helical coiled coil. The majority of coiled-coil structures are based on the 7-residue (heptad) sequence repeat, ***abcdefg***, where ***a*** and ***d*** are usually hydrophobic and the remaining residues tend to be polar.[21–23] When folded, the ***a*** and ***d*** positions of such sequences align along one face of the helix making it amphipathic, Figure 1. Two or more such amphipathic helices assemble through their hydrophobic faces to make the coiled-coil oligomer. Charged residues at ***e*** and ***g***, which flank the ***a/d*** core, are involved in partner selection in hetero-oligomeric assemblies.[24–30] Certain coiled coils—notably, intermediate filaments—extend for tens to hundreds of residues, and, once formed, the basic coiled-coil units assemble or bundle further to form higher-order assemblies and thickened fibers.[31–35] To mimic such a system, we designed the SAF peptides. These comprise two short, complementary peptides engineered to interact and form a 'sticky ended' heterodimer, Figure 2A. The

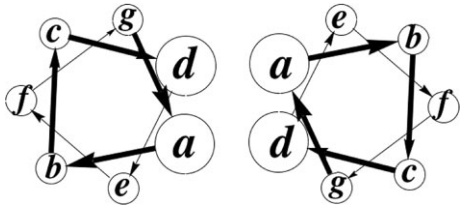

Figure 1. The ***abcdefg*** (heptad) repeat characteristic of coiled-coil protein sequences configured onto α-helical wheels. The α-helix has 3.6 residues per turn. Therefore, hydrophobic residues spaced alternately 3 and 4 residues apart along the chain at ***a*** and ***d*** are brought together to give the helix an apolar face. With the other residues—***b***, ***c***, ***e***, ***f***, and ***g***—largely occupied by polar residues, the overall structure is amphipathic and oligomerizes through the hydrophobic seam. A dimer is shown in this figure, but coiled-coil interfaces with 2, 3, 4, 5, and 12 helices are all known.

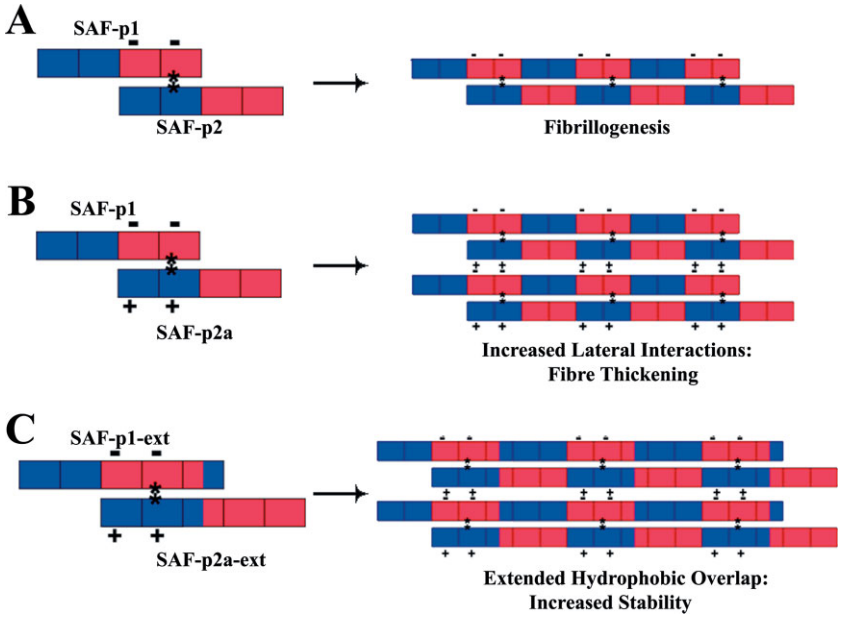

Figure 2. Rational design and redesign of the SAF system. A) In the original, first-generation design, complementary hydrophobic, hydrogen-bonding, and electrostatic interactions were engineered into two peptides, SAF-p1 and SAF-p2, to foster the assembly of sticky-ended dimers, and the formation of long protofibrils. In practice, these protofibrils bundle to give thickened matured fibers [20]. B) In the second-generation redesign, additional positively charged arginines were placed on the surface of SAF-p2a to complement pairs of negatively charged aspartic acid residues on the surface of SAF-p1. The aim was to increase the bundling of protofibrils and, hence, thickening and stability of the fibers. C) In the third generation, an extra heptad was introduced into each peptide to extend their overlap in the sticky-ended dimer and so lead to increased formation and stability of the protofibrils. For simplicity, the schematics emphasize the complementary electrostatic interactions used to drive and cement fiber assembly: blue blocks represent heptads with positively charged lysine residues at the coiled-coil interfacial ***e*** and ***g*** sites; red blocks represent heptads with negatively charged glutamic acid residues at the ***e*** and ***g*** sites; '–' and '+' represent the charged aspartic acid and arginine residues, respectively, on the surfaces of the peptides; and '*' represents complementary buried asparagine residues.

sticky ends are complementary to foster longitudinal assembly of the heterodimers into long coiled-coil fibers. To our knowledge this arrangement of coiled-coil strands is unprecedented in nature, although other research groups have since reported designs for such assemblies.[36–38]

The details of the original, first-generation SAF design are as follows: both SAF peptides are 28-residue, linear peptides comprising proteinogenic amino acids only; to foster coiled-coil dimer formation, the core ***a*** and ***d*** positions are mostly isoleucine and all leucine, respectively;[39,40] each peptide has a basic amino-terminal (N-terminal) half (with ***e*** = ***g*** = Lys) and an acidic carboxy-terminal (C-terminal) half (***e*** = ***g*** = Glu) to promote staggered assembly;[20,25,41] and finally, to cement the stagger further, each peptide has a single asparagine at a different ***a*** site. The significance of these asparagine inclusions is that their amide side chains must be satisfied by hydrogen-bonding interactions when located within a coiled-coil core; placing another complementary asparagine in the partnering coiled-coil strand achieves this and also imparts dimer specificity.[42,43] These first-generation SAFs provided the starting point for the redesigns outlined here.

The first-generation SAF design has been verified experimentally as follows:[20] as judged by circular dichroism (CD) spectroscopy, both SAF peptides are unstructured alone in benign buffer (10 mM MOPS (3-(*N*-morpholino)propane sulfonic acid), pH 7.00), but fold to helical assemblies when mixed at 5 °C; electron microscopy (EM) confirms that the mixtures contain fibers that extend for micrometers in length; and X-ray fiber diffraction confirms α-helical structure running parallel to the long-axis of the fibers.

The SAF system is attractive for biomaterials applications,[1,2] including as scaffolds in TE,[3] because assembly occurs at pH 7 and is effected simply by mixing of two peptide solutions that require no preprocessing. In addition, we have demonstrated that fiber morphology can be altered through rational design, including making peptide-based matrices from the fibers;[44–46] and that functional peptides and proteins can be recruited to the surfaces of the fibers.[47] However, the first-generation fibers have limited utility in such applications because they only assemble up to 15 °C, denature at > 22 °C, and are intolerant to salt. One of the aims of the work presented in this paper was to test if the SAFs could be stabilized through rational redesign. Our starting point was the observation that the first-generation fibers showed thickening similar to the aforementioned natural coiled-coil fibrous intermediate filaments: a typical dimeric α-helical coiled coil is ~2 nm thick; however, matured SAFs are 40–50 nm wide. Therefore, in fibrillogenesis and the maturation process, some lateral assembly must be taking place in addition to the designed longitudinal assembly. In this context we refer to the single 2 nm coiled coil as a 'protofibril'. We sought to test and exploit this to make thicker and potentially more-stable fibers by mutating the sequence of one of the partner peptides to increase protofibril–protofibril interactions, Figure 2. We refer to these peptides and the resulting fibers as 'second-generation SAFs'. In a second redesign iteration we increased the overlap between the two second-generation SAF peptides by adding an extra heptad to each peptide, Figure 1C. This was to increase the length of the hydrophobic overlap between the two peptides in the initial sticky-ended heterodimer and so increase its stability. The rationale here was promote fiber assembly by increasing the population of sticky-ended heterodimers, which we designed as the nucleators and building blocks of the SAFs. We refer to this iteration as 'third-generation' SAF peptides and fibers.

2. Results

2.1. Second-Generation SAFs: Improving Protofibril–Protofibril Interactions

2.1.1. Redesign Principles

Many natural coiled-coil proteins assemble further beyond the primary helix–helix interactions to form higher-order structures and thickened fibers.[48] Coulombic (charge–charge) interactions on the outer surfaces of the helices are often implicated in these processes.[49–51] For example, intermediate-filament proteins initially form two-stranded, parallel coiled coils. These dimers further dimerize themselves into antiparallel tetramers. The tetramers then assemble in a staggered manner to form protofilaments, which bundle to form 10 nm filaments.[48] Alternating patches of basic and acidic amino acids on the surface of the intermediate structures are believed to lie at the heart of this assembly mechanism.[52] Inspired by this, we sought to enhance complementary charged features on the surface of the SAFs' constituent leucine-zipper building blocks to increase lateral fiber assembly. To this end, we modeled contiguous copies of the SAF-p1 and SAF-p2 sequences, Table 1, as an extended dimeric coiled coil, Figure 3A. Inspection of the model suggested that two aspartic acid side chains at consecutive ***b*** sites in the heptad repeat (***abcdefg***), Figure 1, of SAF-p1 formed negatively charged pairs that wound around the surface of the protofibril, Figure 3A and Table 1. Therefore, to introduce complementary positively charged pairs of amino acids, we redesigned SAF-p2 to incorporate two arginine residues,

Table 1. SAF-peptide sequences.

Peptide	Sequence [a]
Heptad repeat	***g abcdefg abcdefg abcdefg abcdefg abcdef***
SAF-p1	K IAALKQK IASLKQE IDALEYE NDALEQ
SAF-p2	K IRALKAK NAHLKQE IAALEQE IAALEQ
SAF-p2a	K IR***R***LK***Q***K NA***R***LKQE IAALE***Y***E IAALEQ
SAF-p1-ext	K IAALKQK IASLKQE IDALEYE NDALEQ***K IAALEQ***
SAF-p2a-ext	K IRRLKQK NARLKQ***K IAALEQ***E IAALEYE IAALEQ

[a] Differences between successive designs are highlighted by bold, italic font.

ADVANCED FUNCTIONAL MATERIALS

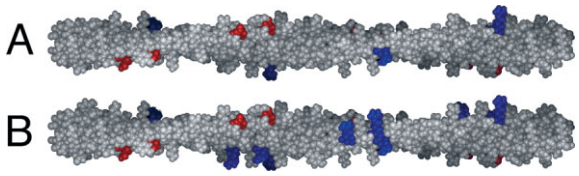

Figure 3. Models for the SAF coiled-coil protofibrils. A) All-atom representation of the 2-stranded coiled-coil model for the originally designed SAF-p1:SAF-p2 assembly. This shows pairs of aspartic acid (red) and single arginine (blue) residues tracking around the surface of the coiled coil. B) A similar model for the redesigned SAF-p1:SAF-p2a assembly in which additional arginine residues were introduced to complement the aspartic acid pairs.

also spaced seven residues apart, at two consecutive ***c*** sites. This resulted in peptide SAF-p2a, Table 1, which we proposed would combine with SAF-p1 to give protofibrils with matching acidic and basic patches on their surfaces, Figure 3B. In turn, these patches could complement each other in protofibril–protofibril interactions to promote lateral higher-order assembly (fiber thickening).

2.1.2. Peptide Assembly

As with the original design, SAF-p1 and SAF-p2a were shown by CD spectroscopy to be unstructured in isolation. However, when mixed, the peptides gave CD spectra with minima at 208 and 222 nm consistent with the formation of considerable α-helix. The precise amount of α-helix could not be gauged because of light scattering from the samples that led to a red-shift of the spectrum and attenuation of the 208 nm signal. This is consistent with our previously reported observations for the original SAF peptides where the α-helical character of the structures was confirmed by X-ray fiber diffraction.[20] The fibrous nature of the assembly was confirmed by transmission electron microscopy (TEM). In comparison to the first-generation fibers, which were slightly curly in appearance under TEM, Figure 4A, the second-generation SAFs gave long straight fibers without bends or kinks, Figure 4C. Moreover, and consistent with the redesign rationale, the second-generation fibers were thicker and better defined than the first-generation: the average fiber width for the second-generation design was 69.2 nm with a standard deviation (s.d.) of 18.5 nm over 113 measurements (n), compared with 43.3 nm (s.d. = 9.3 nm; $n = 195$) for the first-generation SAFs.[20] Clear meridional reflections at 5.15 and 10.3 Å in X-ray fiber diffraction patterns confirmed α-helical coiled coils running parallel to the long axis of the fibers (data not shown).

Finally, and surprisingly, under high magnification, a striation pattern was visible across the widths and along the entire lengths of the second-generation fibers, Figure 4D. This remarkable and novel observation—the first-generation fibers do not show such organization, Figure 4B—warrants further in-depth investigation, which will be presented elsewhere. Briefly, however, fast-Fourier-transform (FFT) analysis of the striations revealed that the lines were separated by 4.23 nm, which corresponds almost exactly to the length expected for a 28-residue SAF peptide fully folded into an α-helical coiled-coil conformation (28×1.48 Å = 4.14 nm). Our working model is that the uranyl acetate, which is generally used as a negative stain for TEM, acts as a positive stain to highlight a regular feature on one of the peptides along the coiled-coil protofibrils, hence the appearance of a striation every peptide unit. One feature that could bind uranyl acetate is the pair of aspartic acid residues at the ***b*** sites in the C-terminal half of SAF-p1, Table 1 and Figure 2. We are currently testing this model and will present the results elsewhere. Most importantly, whatever the origin of the striations, they indicate that the individual peptides and protofibrils within the fiber are aligned and highly ordered in the second-generation fibers, but not in the first.

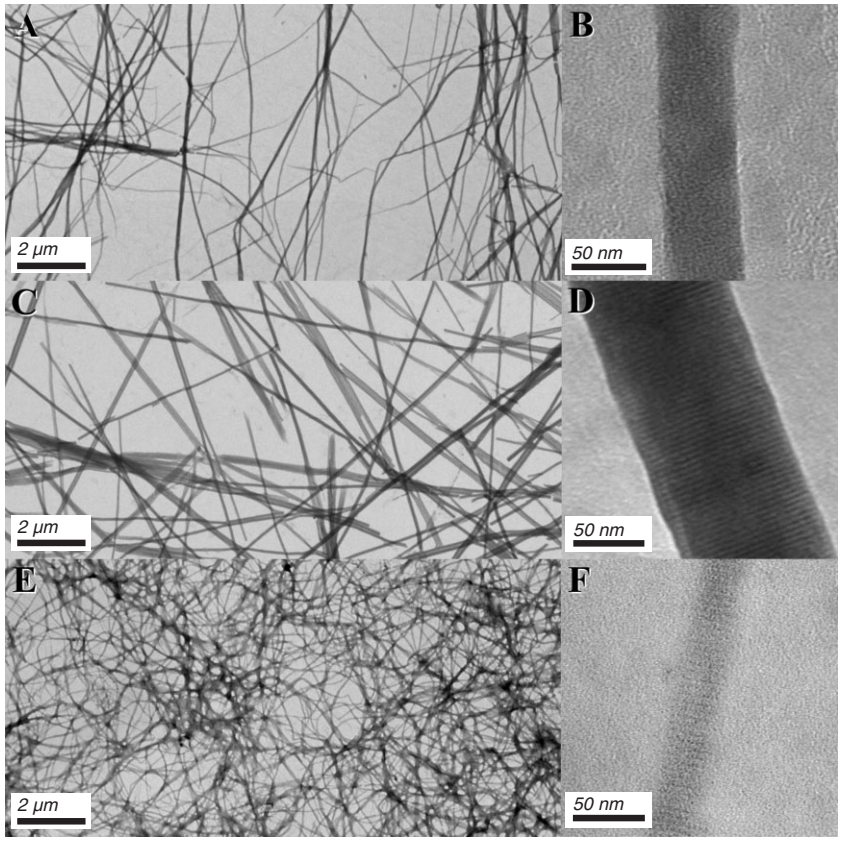

Figure 4. Imaging the stabilized fibers. Low (A) and high (B) magnification electron microscopy images of the first-generation (SAF-p1:SAF-p2) fibers matured for 12 h at 5 °C; second-generation (SAF-p1:SAF-p2a) fibers matured for 12 h at 20 °C (C and D); and for the third-generation (SAF-p1-ext:SAF-p2a-ext) fibers matured for 12 h at 37 °C (E and F). All samples were stained with uranyl acetate.

2.1.3. Stability

As a first step in testing whether the second-generation peptides formed more-stable fibers, the minimum peptide concentration required for assembly was determined. To measure this, the helicity of SAF peptide mixtures at different peptide concentrations was probed by CD spectroscopy. Using this method, the first-generation design had previously been shown to have a critical concentration for assembly of 60 μM; for the second-generation peptides this was found to have improved to 30 μM, Figure 5A.

The helicity of pre-assembled fibers was also followed as a function of temperature to probe the thermal stability of the assembled fibers: first-generation fibers assembled at 5 °C unfold irreversibly with a nominal midpoint of thermal unfolding (T_M) of 22 °C.[20] A similar experiment for the second-generation fibers assembled at 5 °C gave a sigmoidal transition typical of protein unfolding and an improved T_M of 32 °C, Figures 5B and C. Encouraged by the increase in stability, assembly of second-generation fibers was attempted at 22 °C. Interestingly, although assembly was slowed (fibrillogenesis took around 2 h as opposed to 20 min for fibers grown at 5 °C), the thermal stability of the resulting fibers was greater (T_M, 49 °C) than that of fibers grown at 5 °C, Figures 5B and C. This point, that the thermal stability of the fibers can be increased through slowed growth at elevated temperatures, is expanded on in the Discussion. In contrast, although fiber growth was also slowed at elevated temperatures and there was some variation in the midpoint of the unfolding curves for the first-generation fibers formed at 5, 10, and 15 °C, the differences in stability were less dramatic than those observed for the second-generation fibers, Figure 5D, i.e., for the first-generation design, fiber stability could not be improved significantly through slowed growth at higher temperatures.

Finally, the salt tolerances for the first- and second-generation fibers were compared by CD spectroscopy. The first-generation fibers were sensitive to small additions of KCl, with helicity being lost entirely at concentrations of 75 mM and above, Figure 6. In contrast, the helicity of the second-generation was largely unaffected by KCl at up to 100 mM salt, after which structure was lost in a sharp transition, Figure 6.

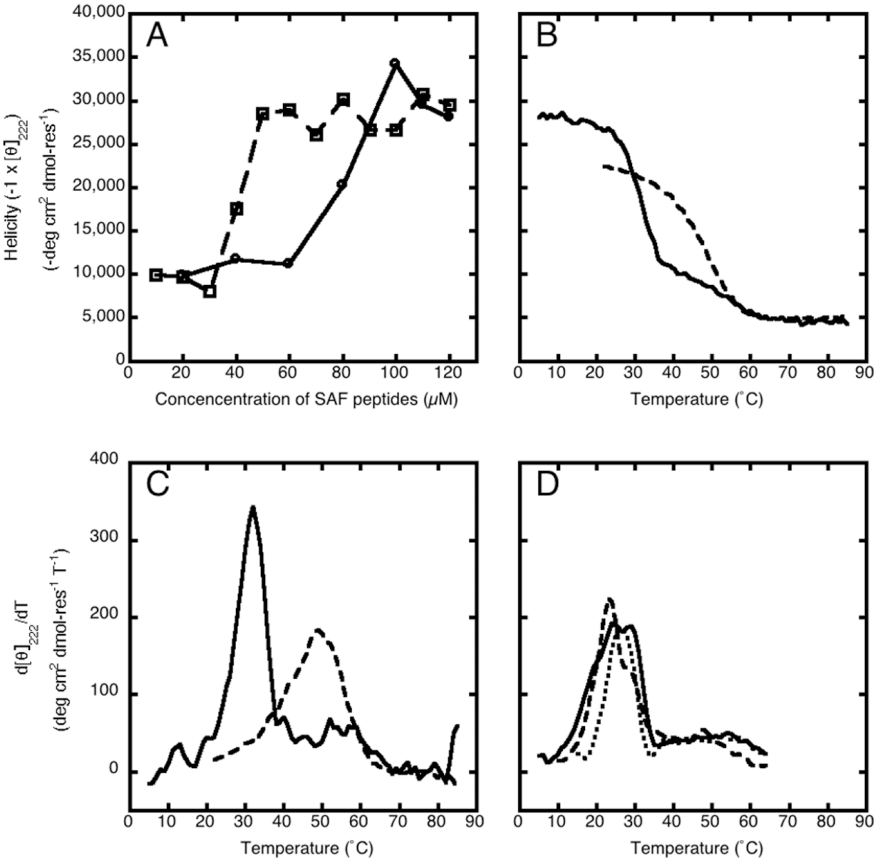

Figure 5. Spectroscopic measurements of fiber formation and stability in solution. A) Helicity—that is, the negative of the CD signal at 222 nm, which provides a measure of coiled-coil structure in solution—plotted against concentration for first-generation fibers (circles and solid line) and the second-generation fibers (squares and broken lines). B) The loss of helicity as a function of temperature for the second-generation fibers prepared at two different temperatures: 5 °C (solid line) and 22 °C (broken line). C) The first derivatives of the plots shown in (A highlighting the midpoints of thermal unfolding. D) A similar analysis to (C but for the first-generation fibers. In this case fibers were grown at 5 °C (solid line), 10 °C (broken line), and 15 °C (dotted line). Conditions for B–D: 100 μM peptide, 10 mM MOPS buffer at pH 7.0.

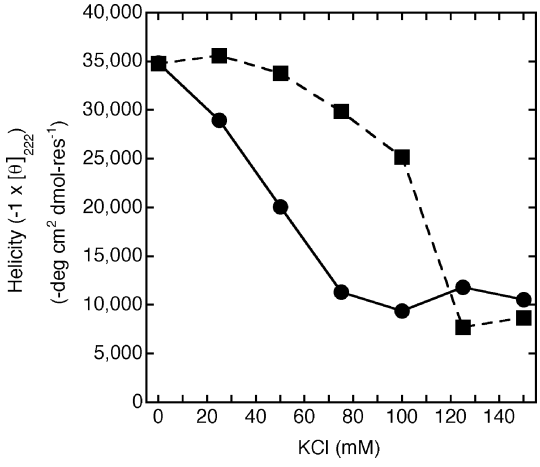

Figure 6. The effect of increasing salt (KCl) on the helical stability of first- (circles and solid line) and second-generation (squares and broken line) SAFs. Conditions: 100 μM peptide; 5 °C; 10 mM MOPS buffer at pH 7.0.

ADVANCED FUNCTIONAL MATERIALS

2.2. Third-Generation SAFs: Increasing the Hydrophobic Overlap

2.2.1. Redesign and Assembly

As previously described, asparagine residues at the ***a*** positions of canonical coiled coils preferentially pair with each other.[42,43,53] This is exploited in the SAF designs by including asparagines at different, complementary heptads in the two peptides in order to prescribe the sticky-ended register of the primary dimer. However, the inclusion of such residues in the hydrophobic core destabilizes coiled-coil structures. In other words, buried asparagines add specificity at the expense of lowered stability. In order to counteract this destabilization, in the third-generation design the asparagine-containing halves of the SAF peptides were extended by one heptad each to give a five-heptad design, Figure 2C, Table 1. Again, CD spectroscopy was used to probe secondary structure. As with both the first- and second-generation designs, third-generation peptides were unstructured in isolation. On mixing, the peptides gave the attenuated and red-shifted α-helical spectrum characteristic of the light scattering caused by the large fibers in solution, Figure 7A.

The third-generation peptides appeared to contain less helix than the second-generation: typical helicity ($-[\theta]_{222}$) values recorded by CD spectroscopy were 25 000–30 000 and 15 000–20 000 deg cm^2 dmol^{-1} for the second and third-generation fibers, respectively. However, the aforementioned light scattering renders accurate comparisons unreliable. As before, fiber assembly was confirmed by TEM, Figure 4E. The third-generation fibers were thinner (58.2 nm, s.d. 9.9 nm, $n = 200$) than those formed by the second-generation peptides. Under high magnification, however, the third-generation fibers were still striated, Figure 4F. This suggests that, despite the thinning and altered morphology of the third-generation fibers, the extra heptads do not disturb the packing of the peptides within the fibers; in other words, that the electrostatic interactions introduced in the second-generation, and maintained in the third, not only continue to cement protofibril–protofibril interactions, but also to specify them. Furthermore, FFT analysis of the third-generation fibers returned a value of 5.23 nm for the separation between striations. This supports our model that the striations are related to the alignment of fully folded α-helical peptide units parallel to the long axis of the fibers; in the case of these peptides, which have 35 amino-acid residues, the length spanned by a fully helical peptide would expected to be 35×1.48 Å $= 5.18$ nm.

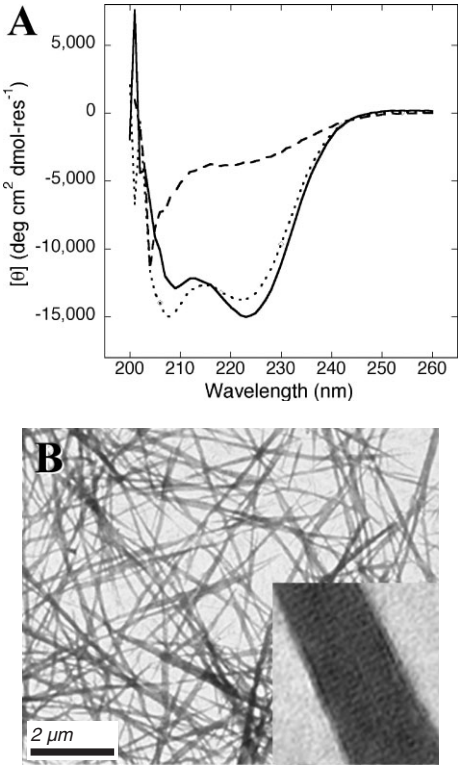

Figure 7. The third-generation fibers in PBS (phosphate-buffered saline). A) CD spectra recorded at 37 °C (solid line), 85 °C (broken line), and 37 °C following cooling from 85 °C (dotted line). B) TEM image of fibers following cooling with striations still visible (insert); the fibers were of comparable size to those observed prior to melting.

The same criteria used to determine the thermal stabilities of the first- and second-generation designs were used to judge the stability of the third-generation fibers. This second iteration of rational redesign resulted in a further increase in stability: for the third-generation designs, fibrillogenesis occurred at up to 37 °C, and T_M rose to 64 °C. Fibrillogenesis at different temperatures did not significantly change the T_M; that is, as with the first generation, stability cannot be improved through slower growth at higher temperatures. The critical concentration for assembly could not be judged by measuring helicity at various peptide concentrations, as it was below 10 μM and the limits of reliable CD measurements. Consequently, the critical concentration was determined by TEM as follows: samples were prepared over a range of peptide concentrations from 10–2 μM; TEM images were recorded, Figure 8, and the critical concentration was taken as the lowest peptide concentration that gave visible fibers—this was found to be 4 μM.

2.2.2. Tolerance to Salt

One aim of the rational redesign of the SAFs is to increase their stability sufficiently for assembly in cell culture. As a prelude to such experiments, and to mimic physiological conditions of pH, salt concentration, and temperature, assembly of the third-generation SAFs was investigated in phosphate-buffered saline (PBS, 150 mM NaCl) and at 37 °C; neither the first- nor second-generation fibers assembled at this concentration of salt at any temperature, Figure 6. Under these conditions, the third-generation SAF mixtures gave α-helical spectrum with the attenuation of the signal at 208 nm and red-shift characteristic of standard SAF preparations, Figure 7A. Furthermore, following thermal unfolding and cooling back to 37 °C, complete recovery of signal was observed, and the presence of fibers was confirmed by TEM, Figure 7B. The fibers reformed their original morphology and striation patterns after cooling. This is interesting, as it shows that thermal unfolding of the

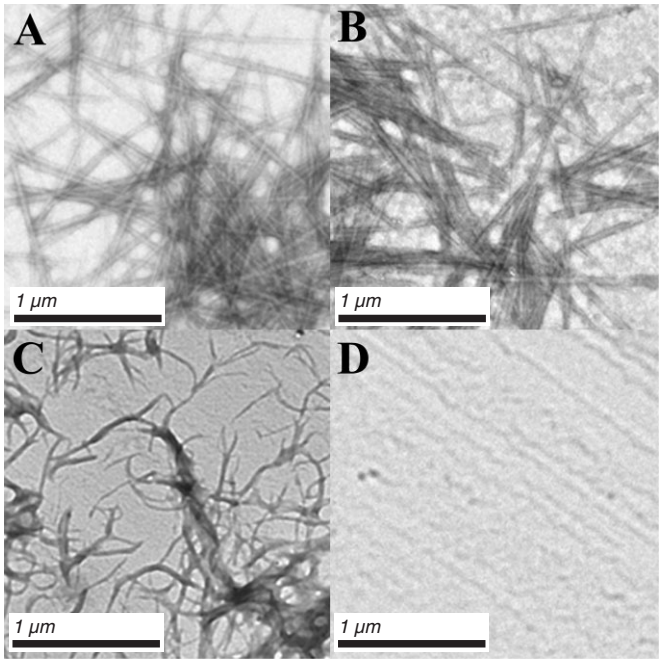

Figure 8. Critical concentration for assembly of the third-generation fibers determined by TEM. Images of third-generation peptide mixtures at A) 10 μM, B) 6 μM, C) 4 μM, and D) 2 μM.

third-generation SAFs is reversible in PBS. This contrasts with the behavior of the earlier SAF designs, which do not reassemble after thermal denaturation in more benign buffers.

It is important for TE applications that fibers persist for sufficient time for cells to attach and to begin to produce their own matrix. To probe the longevity of fibers in salt-containing solutions at 37 °C, TEM images were recorded 24 h and 4 and 8 days after mixing. These revealed that the fibers were stable for prolonged periods under these conditions, although inspection of the images recorded at up to one month after mixing showed the matured fibers beginning to bundle.

With these results we have achieved our aim of producing fibers that are not only stable, but also self-assemble, under conditions of physiological pH, temperature, and ionic concentration.

3. Discussion and Conclusions

Through two iterations of rational peptide redesign we have succeeded in considerably stabilizing the assembly and structure of a designed protein fibrous material (SAF) in aqueous buffers. Specifically, the original (first-generation) design could only be assembled at up to 15 °C, at around pH 7 and without salt. Our aim was to promote assembly and increase stability of the fibers for applications requiring conditions around 37 °C, pH 7, and at physiological salt concentrations. The two rational redesign steps were: 1) to promote fiber thickening through improved electrostatic interactions between the nascent protofibril chains; 2) to improve the initial step in fibrillogenesis—namely, the formation of a sticky-ended peptide dimer—by making the component peptides longer, thus increasing their overlap and the hydrophobic interaction between them. Consistent with this redesign rationale, compared with the first-generation structures the second-generation were thicker, and both the second- and third-generation fibers formed more rapidly and at lower peptide concentrations. Furthermore, the second- and third-generation fibers could be assembled at pH 7 at up to 22 °C and above 37 °C, respectively; and at up to 100 mM salt and above 250 mM salt, respectively.

Two interesting and novel features of the SAF system also emerged from the redesign process. In contrast to the first-generation fibers, which are long cylindrical structures devoid of surface features, both of the redesigned fibers show clear striation patterns that run straight across the fibers perpendicular to the long fiber axis. These nanoscale features persist for tens of micrometers along the lengths of the fibers. Moreover, the distances between striations—second generation, 4.23 nm; third generation, 5.23 nm—almost precisely match the expected lengths of the designed SAF peptides configured in α-helical conformations. This strongly suggests that the peptide building blocks of the fibers are aligned end-to-end along the long axis of the fibers, and side-by-side across their widths. A full structural analysis of these fibers will be presented elsewhere. Briefly, however, we note that similar nanoscale features are evident in other natural protein systems such as collagens,[48] and, more recently, in designed peptide[54] and DNA[55] systems. In these systems, like ours, the striation patterns reflect the underlying molecular building blocks of the assemblies.

The other notable feature of the second-generation fibers is that their stability can be improved by growth at higher temperatures, at least up to the point where the peptides no longer fold and assemble. Briefly, when grown at 5 °C the midpoint of thermal unfolding (T_M) of the fibers is 32 °C; and when grown at 22 °C the unfolding transition is cleaner and the T_M improved to 40 °C. 'Cleaner' refers to the fact that the unfolding transition for the higher-temperature preparation is sigmoidal indicative of cooperative unfolding, whereas that for the lower-temperature preparation, although initially sharper, has a broad tail suggestive of a second unfolding process. Interestingly, and consistent with this, fibers grown at an intermediate temperature, 15 °C, gave an unfolding profile with two distinct populations with similar T_M values for fibers grown at 5 and 22 °C.[56] These data indicate that there are at least two types of fiber present in some of the preparations, and that the population of each type depends on the conditions. In strong support of this, although mixed populations of striated and smooth fibers are observed to some extent for all preparations of second-generation fibers, those prepared at 22 °C are striated more frequently and more clearly than those prepared at lower temperatures. In summary, these results indicate that fiber morphology and stability is determined to some extent by the conditions (in this case, temperature) under which the fibers are prepared. This is interesting and it provides another route for altering and even tailoring the properties of the self-assembled fibers. For the second-generation designs, the best-defined and most-stable fibers are formed slowly at 22 °C.

ADVANCED FUNCTIONAL MATERIALS

Why do more-stable and better-ordered fibers result when second-generation fibers are assembled at higher temperatures? The most straightforward explanation of this is as follows: first, we assume that all of the processes leading up to fiber formation—namely, sticky-ended heterodimer formation, fiber elongation into protofibrils, and protofibril association to form fibers—are reversible protein-folding and assembly events. Thus, any misfolding event, which could ultimately lead to a defect (or less regularity) in the fiber—for instance, the incorporation of an incorrect or misaligned peptide—could be reversed by one or more of the reverse (disassembly and unfolding) reactions. Although raising the temperature increases the rates of the forward (folding and assembly) reactions, it does the same to these reverse reactions. Thus, at higher temperatures, correction of misfolding and potential defects will be faster; in other words, there is less opportunity for aberrant interactions to become kinetically trapped.

One point that needs clarification in this proposed mechanism is the observation that the overall rate of fibrillogenesis is slowed at higher temperatures. This seems counterintuitive because all of the rates should increase with temperature. However, peptide folding and assembly processes have significant change in entropy (ΔS) terms that favor the reverse (unfolding and disassembly) reactions. Thus, their overall equilibrium positions will shift to the unfolded side with increased temperature. In other words, the pools of productive species—the sticky-ended heterodimers and protofibrils—that lead to fibrillogenesis will be reduced at higher temperatures, and the overall rate of fibrillogenesis will be slowed.

Our observations fit with this proposed mechanism: for 60 or 100 μM second-generation peptide mixtures at 5 °C maturation to thick fibers took ca. 20 min; note that the rates of fibrillogenesis showed the expected concentration dependence with half times ($t_{1/2}$) of approximately 10 and 2 min, respectively, for these two concentrations. In contrast, at 22 °C the processes took >2 h. As stated above, fibers grown at 22 °C showed better morphology and clearer striations. In essence, this is similar to many other systems in which slowed growth leads to better-ordered and more-stable cooperative assemblies.

Perhaps surprisingly, the stability of the third-generation fibers could not be improved similarly by raising the temperature and slowing growth; it is possible that, for this design iteration, assembly is so rapid that it is not influenced significantly by the relatively small temperature range that can be examined in aqueous solution; indeed, fibrillogenesis of the third-generation fibers is rapid (ca. 20 min) at all temperatures. Nevertheless, the third-generation fibers assemble and are stable above 37 °C in physiological salt at pH 7.

The results that we have presented are extremely encouraging for our overall goal of achieving the rational design of a biocompatible peptide-based scaffold for in vivo applications in 3D cell culture and tissue engineering. Experiments are now in progress in our laboratory to assess the assembly of the third-generation SAFs in cell-culture media, and how cells respond to this new biomaterial. Moreover, the success of this rational design approach that we describe bodes well for the challenge of rationally designing nanostructured soft materials from the bottom up.[1,2,19] The potential applications of peptide-based fibrous systems do of course extend beyond the development of scaffolds for 3D cell culture and tissue engineering.[3] Specifically, other applications could include preparing modified biocompatible surfaces, making responsive materials, and as self-assembled templates for the organized growth of organic and inorganic materials.[1,2]

4. Experimental

Model Building: Models for the SAF protofibrils were made as follows: the coiled-coil backbone was generated by a program, NONCRICKCC [57], using standard coiled-coil parameters (every seventh residue equivalent; pitch, 144 Å; helix spacing, 8.9 Å); side chains were added in InsightII (MSI, San Diego, CA) using favored rotamers for side chains in the α-helix. The models were soaked in a 5 Å layer of water and energy minimized using 100 steps of steepest decent in the CVFF force field.

Peptide Synthesis: Peptides were made chemically on a Pioneer Peptide Synthesis System (PE Applied Biosystems, CA, USA) using standard Fmoc-based solid-phase protocols (Fmoc = 9-fluorenylmethyloxycarbonyl). Peptides were purified by semi-preparative reverse-phase high-pressure liquid chromatography (RP-HPLC). The final constructs were identified by matrix-assisted laser ionization desorption time-of-flight (MALDI-TOF) mass spectrometry (Micromass Ltd, Manchester, UK). MS [*M*+H] +: SAF-p1: *m*/*z* 3174 (calc), 3175 (found); SAF-p2: *m*/*z* 3128 (calc), 3129 (found); SAF-p2a: *m*/*z* 3325 (calc), 3326 (found); SAF-p1-ext: *m*/*z* 3927 (calc), 3928 (found); SAF-p2a-ext: *m*/*z* 4079 (calc), 4080 (found). Peptide concentrations were determined by UV spectroscopy assuming an ε_{280} of 1280 M^{-1} cm^{-1} for tyrosine.

Circular Dichroism (CD) Spectroscopy: CD spectra and melts were recorded as described previously [20] except that 1, 0.5, 0.2, and 0.1 cm cuvettes were used to cover peptide concentration ranges used. For the thermal denaturation experiments 0.1 cm cuvettes were used; solutions were incubated at 5, 10, 15, 22, or 37 °C (see text for details for each generation) for between 2 and 12 h as indicated in the text prior to the melts; and the following spectrometer settings were employed: a 1 nm slit width, a 4 s response time, and a ramping rate of 0.5 °C per minute for thermal melts.

Electron Microscopy: Samples for TEM were prepared and images recorded as described previously [20]. With the exception of the TEM experiments performed to determine the critical concentration for assembly of the third-generation SAFs, for which peptide concentrations are given in the text, the final concentration of each SAF peptide was 100 μM. Fiber widths were measured on images recorded at 1000× magnification using the straight-line selection tool of imageJ [58]. The third-generation fibers prepared in PBS were stained using ammonium dimolybdate.

Received: August 24, 2005
Final version: November 29, 2005
Published online: April 10, 2006

[1] C. E. MacPhee, D. N. Woolfson, *Curr. Opin. Solid State Mater. Sci.* **2004**, *8*, 141.
[2] R. Fairman, K. S. Akerfeldt, *Curr. Opin. Struct. Biol.* **2005**, *15*, 453.
[3] M. M. Stevens, J. H. George, *Science* **2005**, *310*, 1135.
[4] K. F. Leong, C. M. Cheah, C. K. Chua, *Biomaterials* **2003**, *24*, 2363.
[5] S. J. Shieh, J. P. Vacanti, *Surgery* **2005**, *137*, 1.
[6] C. E. Semino, *J. Biomed. Biotechnol.* **2003**, *2003*, 164.
[7] V. L. Tsang, S. N. Bhatia, *Adv. Drug Delivery Rev.* **2004**, *56*, 1635.
[8] Z. Ma, M. Kotaki, R. Inai, S. Ramakrishna, *Tissue Eng.* **2005**, *11*, 101.
[9] M. G. Ryadnov, B. Ceyhan, C. M. Niemeyer, D. N. Woolfson, *J. Am. Chem. Soc.* **2003**, *125*, 9388.
[10] A. Abbott, *Nature* **2003**, *424*, 870.

[11] R. Langer, D. A. Tirrell, *Nature* **2004**, *428*, 487.
[12] A. Persidis, *Nat. Biotechnol.* **1999**, *17*, 508.
[13] T. C. Holmes, S. De Lacalle, X. Su, G. Liu, A. Rich, S. Zhang, *Proc. Natl. Acad. Sci. USA* **2000**, *97*, 6728.
[14] J. D. Hartgerink, E. Beniash, S. I. Stupp, *Proc. Natl. Acad. Sci. USA* **2002**, *99*, 5133.
[15] J. D. Hartgerink, E. Beniash, S. I. Stupp, *Science* **2001**, *294*, 1684.
[16] G. A. Silva, C. Czeisler, K. L. Niece, E. Beniash, D. A. Harrington, J. A. Kessler, S. I. Stupp, *Science* **2004**, *303*, 1352.
[17] J. K. Kretsinger, L. A. Haines, B. Ozbas, D. J. Pochan, J. P. Schneider, *Biomaterials* **2005**, *26*, 5177.
[18] T. C. Holmes, *Trends Biotechnol.* **2002**, *20*, 16.
[19] S. Zhang, *Nat. Biotechnol.* **2003**, *21*, 1171.
[20] M. J. Pandya, G. M. Spooner, M. Sunde, J. R. Thorpe, A. Rodger, D. N. Woolfson, *Biochemistry* **2000**, *39*, 8728.
[21] F. H. C. Crick, *Acta Crystallogr.* **1953**, *6*, 689.
[22] J. Walshaw, D. N. Woolfson, *J. Mol. Biol.* **2001**, *307*, 1427.
[23] A. N. Lupas, M. Gruber, *Adv. Protein Chem.* **2005**, *70*, 37.
[24] E. K. O'Shea, R. Rutkowski, W. F. Stafford, III, P. S. Kim, *Science* **1989**, *245*, 646.
[25] E. K. O'Shea, R. Rutkowski, P. S. Kim, *Cell* **1992**, *68*, 699.
[26] E. J. Spek, A. H. Bui, M. Lu, N. R. Kallenbach, *Protein Sci.* **1998**, *7*, 2431.
[27] N. E. Zhou, C. M. Kay, R. S. Hodges, *Protein Eng.* **1994**, *7*, 1365.
[28] O. D. Monera, N. E. Zhou, C. M. Kay, R. S. Hodges, *J. Biol. Chem.* **1993**, *268*, 19 218.
[29] O. D. Monera, C. M. Kay, R. S. Hodges, *Biochemistry* **1994**, *33*, 3862.
[30] K. S. Thompson, C. R. Vinson, E. Freire, *Biochemistry* **1993**, *32*, 5491.
[31] A. D. McLachlan, J. Karn, *J. Mol. Biol.* **1983**, *164*, 605.
[32] G. N. Phillips, Jr., *J. Mol. Biol.* **1986**, *192*, 128.
[33] D. A. Marvin, *Curr. Opin. Struct. Biol.* **1998**, *8*, 150.
[34] E. M. De La Cruz, A. Mandinova, M. O. Steinmetz, D. Stoffler, U. Aebi, T. D. Pollard, *J. Mol. Biol.* **2000**, *295*, 517.
[35] H. Herrmann, U. Aebi, *Annu. Rev. Biochem.* **2004**, *73*, 749.
[36] S. Kojima, Y. Kuriki, T. Yoshida, K. Yazaki, K. Miura, *Proc. Jpn. Acad. Ser. B* **1997**, *73*, 7.
[37] A. V. Kajava, S. A. Potekhin, G. Corradin, R. D. Leapman, *J. Pept. Sci.* **2004**, *10*, 291.
[38] Y. Zimenkov, V. P. Conticello, L. Guo, P. Thiyagarajan, *Tetrahedron* **2004**, *60*, 7237.
[39] P. B. Harbury, T. Zhang, P. S. Kim, T. Alber, *Science* **1993**, *262*, 1401.
[40] D. N. Woolfson, T. Alber, *Protein Sci.* **1995**, *4*, 1596.
[41] S. Nautiyal, D. N. Woolfson, D. S. King, T. Alber, *Biochemistry* **1995**, *34*, 11 645.
[42] K. J. Lumb, P. S. Kim, *Biochemistry* **1995**, *34*, 8642.
[43] L. Gonzalez, Jr., D. N. Woolfson, T. Alber, *Nat. Struct. Biol.* **1996**, *3*, 1011.
[44] M. G. Ryadnov, D. N. Woolfson, *Angew. Chem. Int. Ed.* **2003**, *42*, 3021.
[45] M. G. Ryadnov, D. N. Woolfson, *Nat. Mater.* **2003**, *2*, 329.
[46] M. G. Ryadnov, D. N. Woolfson, *J. Am. Chem. Soc.* **2005**, *127*, 12 407.
[47] M. G. Ryadnov, D. N. Woolfson, *J. Am. Chem. Soc.* **2004**, *126*, 7454.
[48] T. D. Pollard, W. C. Earnshaw, *Cell Biology*, Saunders, London **2002**.
[49] D. A. Parry, W. G. Crewther, R. D. Fraser, T. P. MacRae, *J. Mol. Biol.* **1977**, *113*, 449.
[50] D. A. Parry, *Guidebook to the Cytoskeletal and Motor Proteins*, Oxford University Press, Oxford, UK **1999**.
[51] A. D. McLachlan, M. Stewart, *J. Mol. Biol.* **1982**, *162*, 693.
[52] J. J. Meng, S. Khan, W. Ip, *J. Biol. Chem.* **1994**, *269*, 18 679.
[53] E. K. O'Shea, J. D. Klemm, P. S. Kim, T. Alber, *Science* **1991**, *254*, 539.
[54] E. T. Powers, S. I. Yang, C. M. Lieber, J. W. Kelly, *Angew. Chem. Int. Ed.* **2002**, *41*, 127.
[55] J. C. Mitchell, J. R. Harris, J. Malo, J. Bath, A. J. Turberfield, *J. Am. Chem. Soc.* **2004**, *126*, 16 342.
[56] A. M. Smith, *D.Phil. Thesis*, University of Sussex, UK **2003**.
[57] G. Offer, M. R. Hicks, D. N. Woolfson, *J. Struct. Biol.* **2002**, *137*, 41.
[58] M. D. Abramoff, P. J. Magelhaes, S. J. Ram, *Biophotonics Int.* **2004**, *11*, 36.